Two-dimensional tunneling in a SQUID

B. Ivlev[1] and J. P. Palomares-Báez[2]
[1]*Instituto de Física, Universidad Autónoma de San Luis Potosí, San Luis Potosí, San Luis Potosí 78000, Mexico*
[2]*Instituto Potosino de Investigación Cientifica y Tecnológica, San Luis Potosí, San Luis Potosí 78231, Mexico*
(Received 6 April 2010; revised manuscript received 23 October 2010; published 9 November 2010)

Traditionally quantum tunneling in a superconducting quantum interference device (SQUID) is studied on the basis of a classical trajectory in imaginary time under a two-dimensional potential barrier. The trajectory connects a potential well and an outer region crossing their borders in perpendicular directions. In contrast to that main-path mechanism, a wide set of trajectories with components tangent to the border of the well can constitute an alternative mechanism of multipath tunneling. The phenomenon is essentially nonone-dimensional. Continuously distributed paths under the barrier result in enhancement of tunneling probability. A type of tunneling mechanism (main path or multipath) depends on character of a state in the potential well prior to tunneling. A temperature dependence of the tunneling probability in a very asymmetric (different capacitances) SQUID has a finite slope at zero temperature. A transition between thermally assisted tunneling and pure activation can be not smooth depending on current through a very asymmetric SQUID.

DOI: 10.1103/PhysRevB.82.184513 PACS number(s): 85.25.Dq, 74.50.+r

I. INTRODUCTION

Phases in Josephson junctions[1] are usually treated as macroscopic degrees of freedom. However they can exhibit quantum properties.[2] In particular, quantum tunneling of those variables across a potential barrier is possible.[3–6] Tunneling in a single Josephson junction is similar to a conventional one-dimensional quantum-mechanical process. In this case the tunneling mechanism is described by theory of Wentzel, Kramers, and Brillouin (WKB).[7–10] Tunneling occurs from a classically allowed region which is a conventional potential well where energy levels are quantized.[11–14] Quantum coherence between potential wells was demonstrated.[15–18]

Besides single Josephson junctions, superconducting quantum interference devices (SQUID) are also a matter of active investigation for many years.[19–27] A SQUID consists of two Josephson junctions and, therefore, represents a two-dimensional system where macroscopic quantum tunneling is also possible. Tunneling in multidimensional systems is well studied.[28–32] There is the certain underbarrier path (or a few paths) where a wave function is localized and it decays along the path. This main-path tunneling is described by a classical trajectory in imaginary time and it is analogous to a conventional WKB mechanism.

In contrast to that, a different scenario of tunneling in a static SQUID is possible. Instead of localization on a main path an underbarrier state is distributed over a continuous set of paths. Multipath tunneling cannot be described in terms of a classical trajectory in imaginary time.

A realization of a particular tunneling mechanism (main path or multipath) depends on type of a state in the potential well prior to tunneling. Suppose, in the classical treatment, a state in a well has a momentum component orthogonal at some point to a border of the well (a normal reflection). The main path starts at that point and continues under the barrier. When a state in the well has also a component which is tangent to the border at some point (a particle hits the border from some angle) a scenario is different. Around that point there a set of continuously distributed classical paths which go under the barrier.

The first goal of the paper is to propose a different aspect of tunneling in a static SQUID, which is a multipath mechanism. These results are presented in Ref. 33. See also Ref. 34. The phenomenon is essentially nonone-dimensional and it occurs in a SQUID which is symmetric or at least not very asymmetric. As shown in the paper, a multipath mechanism can result in a larger probability of tunneling compared to main path. Different paths interfere and a method of classical trajectory in imaginary time, in contrast to main path, is not valid. In experiments it is possible to determine a contribution of multipath effects to a total probability of tunneling. A dc SQUID in zero magnetic field and without dissipation is considered in the paper.

In Sec. II a formulation of the problem is given. In Sec. III general arguments are used to explain multipath phenomenon and to estimate the effect. It is shown that multipath tunneling through a two-dimensional static barrier in a not very asymmetric SQUID is analogous to photon-assisted tunneling across a nonstationary one-dimensional barrier. In Sec. IV an exact solution of the semiclassical problem is done with the use of a certain model coupling between the junctions in a symmetric SQUID. The exact calculations confirm the estimate of the effect performed on the basis of general arguments in Sec. III.

The second goal of the paper is to study tunneling in a very asymmetric SQUID. Capacitances of two junctions in a SQUID play a role of masses. When one capacitance is large the masses become very different and one phase becomes "heavy." This provides an additional interest for study of an asymmetric SQUID. A behavior of an asymmetric SQUID after tunneling was investigated.[27]

During tunneling process a motion along the heavy coordinate is weakly generated and the process of barrier crossing becomes almost one-dimensional when the heavy phase is fixed. This fixed value should be determined from a condition of maximum of a tunneling probability.

That program has been performed in the paper. There are two unusual features of results.

First, the tunneling probability, as a function of temperature, has a finite slope at low temperature. This contrasts to a temperature dependence for a one-dimensional barrier where that slope is zero.

Second, a transition at a finite temperature between thermally assisted tunneling and pure activation changes its character when current approaches the critical value. At those currents temperature dependence of tunneling probability exhibits a finite jump of slopes at the transition temperature. When current is not too close to the critical value the transition is smooth as for a one-dimensional barrier.

In Sec. VI we apply to a SQUID a semiclassical formalism of Hamilton-Jacobi. In Sec. VII the method of classical trajectories in imaginary time is used which accounts for an optimization of tunneling probability with respect to a value of the heavy phase. In Sec. X it is argued that experimental observations of the proposed phenomena in a SQUID are real.

II. FORMULATION OF THE PROBLEM

We consider a dc SQUID, consisting of two Josephson junctions with phases φ_1 and φ_2 with no dissipation when the two junctions are inductively coupled. Critical currents of the junctions are equal but capacitances C_1 and C_2 can be different. We define the asymmetry parameter

$$M = \frac{C_2}{C_1}. \tag{1}$$

A classical behavior of phases corresponds to conservation of the total energy

$$E_0 = \frac{E_J}{2\omega^2}\left[\left(\frac{\partial\varphi_1}{\partial t}\right)^2 + M\left(\frac{\partial\varphi_2}{\partial t}\right)^2\right] + E_J\left[-\cos\varphi_1 - \cos\varphi_2 - j(\varphi_1+\varphi_2) + \frac{1}{2\beta}(\varphi_1-\varphi_2)^2\right], \tag{2}$$

where the dimensionless current $j=I/2I_c$, the Josephson energy $E_J=\hbar I_c/2e$, the plasma frequency $\omega=\sqrt{2eI_c/\hbar C_1}$, and the coupling parameter $\beta=2\pi LI_c/\Phi_0$ are introduced. Here I_c and L are critical current and inductance of each individual junction. The magnetic flux quantum is $\Phi_0=\pi\hbar c/e$.

Below we consider large β and the total current I close to its critical value, $(1-j)\ll 1$. New variables are introduced by the relations

$$\varphi_1 = \frac{\pi}{2} + (3x-1)\sqrt{2(1-j)} + \frac{3x}{\beta},$$

$$\varphi_2 = \frac{\pi}{2} + (3y-1)\sqrt{2(1-j)} + \frac{3y}{\beta}. \tag{3}$$

Time is measured in the unit of

$$t_0 = \frac{\sqrt{2\beta}}{\omega}\sqrt{\frac{\alpha}{1+\alpha}}, \tag{4}$$

where the coupling parameter is

$$\alpha = \frac{1}{\beta\sqrt{2(1-j)}}. \tag{5}$$

The energy in Eq. (2) takes the form

$$E_0 = \frac{\hbar B}{t_0}\left[\frac{1}{2}\left(\frac{\partial x}{\partial t}\right)^2 + \frac{M}{2}\left(\frac{\partial y}{\partial t}\right)^2 + V(x,y)\right], \tag{6}$$

where

$$B = \frac{B_0}{\sqrt{2}}\left(\frac{1+\alpha}{\alpha}\right)^{5/2}, \quad B_0 = \frac{9E_J}{\hbar\omega\beta^{5/2}}. \tag{7}$$

The potential energy is

$$V(x,y) = V_0(x) + V_0(y) - \frac{2\alpha xy}{1+\alpha}, \tag{8}$$

where $V_0(x)=x^2-x^3$. B in Eq. (6) is called semiclassical parameter. When B is large the phase dynamics is mainly classical. Below we consider that case, $1\ll B$.

A classical dynamics of phases in a SQUID corresponds to Eqs. (6) and (8). The effective particle moves in the classically allowed region (in a vicinity of the point $x=y=0$) which is restricted by the potential barrier. As known, the particle can tunnel through the barrier resulting in experimentally observable phase jumps. A tunneling scenario, as shown in the paper, substantially depends on the asymmetry parameter M.

III. TUNNELING IN A SYMMETRIC SQUID

Below, in Secs. III–V, we consider a symmetric SQUID, $M=1$. The conclusions drawn relate also to the case of a not very asymmetric SQUID, $M\sim 1$.

A character of tunneling depends on coupling strength α between the two junctions. When the coupling is strong, $1\ll\alpha$, one can easily show that the last term in the energy [Eq. (2)] dominates.[20] Therefore in this case the particle tunnels along the direction $x=y$ since fluctuations around this path cost a large energy. In contrast, at a small coupling, $\alpha\ll 1$, the junctions are almost independent and there are two different tunneling paths, along the x or y direction.[20]

As follows, at a very strong and a very weak coupling between two junctions the system behaves as effectively one-dimensional. Essential features of two dimensions are exhibited for an intermediate coupling, $\alpha\sim 1$. Below we study a formation of that regime starting from a region of small α.

A. Uncoupled junctions

Let us consider first zero coupling between two junctions ($\alpha=0$). In this case Eqs. (6) and (8) describe two independent particles in one-dimension potentials shown in Fig. 1. When the semiclassical parameter B is large the potential barriers in Fig. 1 are hardly transparent and a number of discrete levels in the wells is large.

Suppose tunneling to occur in the x direction. We introduce the dimensionless energy E

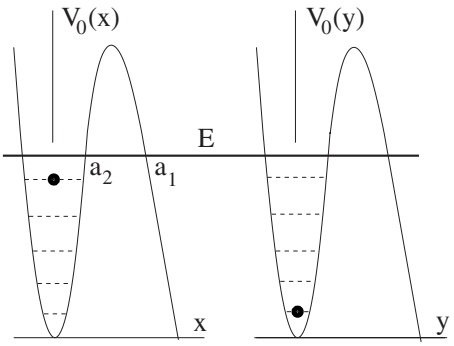

FIG. 1. Uncoupled junctions, $\alpha=0$. The total particle energy E is fixed. The maximum tunneling probability in the x direction relates to a maximum excitation of the y motion to provide a maximum energy in the x direction.

$$E_0 = \frac{\hbar B}{t_0} E. \tag{9}$$

The total particle energy E in Fig. 1 is a sum of ones corresponding to motions in the x and y directions. A maximal tunneling probability of a particle, with a fixed total energy E, is realized when the energy of the x motion has a maximal possible value. This situation is shown in Fig. 1. In this case a motion in the direction perpendicular to tunneling (the y direction) is not excited pertaining to a lowest level in y. In the classical treatment, the particle hits a border of the well, $V(x,y)=E$, with zero tangent velocity.

For comparison, in Fig. 2 the total energy E is distributed in a way that the y motion is excited. In the classical treatment, the particle hits a border of the well with a finite tangent velocity. This results in less probable tunneling in the x direction since tunneling occurs from a lower level, $E-\delta E$, as shown in Fig. 2. The part δE of the total energy relates to the tangent motion.

B. Weakly coupled junctions

Suppose the junctions are weakly coupled so that $\alpha \ll 1$. In this case a motion in the total potential [Eq. (8)] cannot be reduced to two independent ones as in Figs. 1 and 2. Now the entire system of levels in the total potential [Eq. (8)]

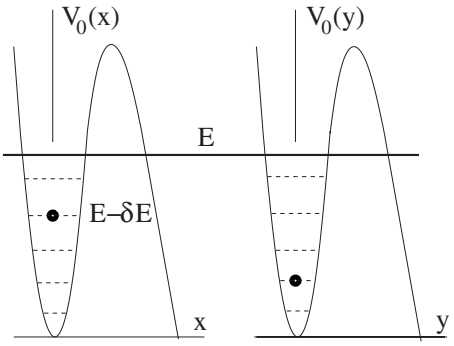

FIG. 2. Uncoupled junctions, $\alpha=0$. A part of the total energy E is given up to an excitation of the y motion resulting in a reduced tunneling probability in the x direction compared to Fig. 1.

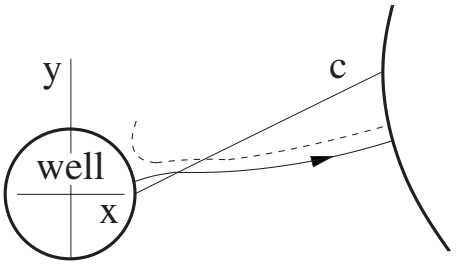

FIG. 3. At $\delta E=0$ the main path (arrowed curve) connects two classically allowed domains, the potential well and the outer region. The thick curves relate to the condition $V(x,y)=E$. A deviation from the main path (dashed curve) does not lead to the well. On the line c the y component of a force is zero, $\partial V/\partial y=0$.

accumulates the levels of the x and y channels in Fig. 1. If there are five discrete levels in each well, $V_0(x)$ and $V_0(y)$, then the potential $V(x,y)$ contains 25 levels.

Let us analyze specificity of two-dimensionality in tunneling. First, the coupling constant α is partly accounted for in the parameter B in Eq. (7). At a small α this leads to a linear in α reduction of tunneling probability. The last term in the potential [Eq. (8)] is proportional to α^2 since $y \sim \alpha$. So we calculate an α^2 correction to the tunneling probability. It is small at $\alpha \ll 1$ but it becomes significant at $\alpha \sim 1$.

Below in this section we propose some nonrigorous arguments which help to understand what happens under the barrier in two dimensions. When a particle hits a border of the well with zero tangent momentum, $\delta E=0$, an underbarrier wave function is localized on the certain classical trajectory which is orthogonal to the borders of classical regions.[28–32] This trajectory is shown in Fig. 3 by the arrowed curve. The trajectory is driven by the y force directed away form the line $y=\alpha x/(1+\alpha)$ where it changes sign. That line is marked in Fig. 3 as c. Not far from the outer region the x force, $\partial V/\partial x$, attracts the particle to the line c as it is tilted.

A wave function is proportional to $\exp(iS/\hbar)$ where S is a classical action.[10] According to Maupertuis' principle,[35] along the classical trajectory one should put $S=S_{cl}$, where

$$S_{cl} = i\hbar B \int dl \sqrt{V(x,y) - E} \tag{10}$$

and dl is an element of the classical trajectory. This mechanism can be called main path tunneling since another path does not lead to the well in Fig. 3 deviating from it as the classical trajectory shown by the dashed curve.[30,31] Equation (10) is analogous to a conventional WKB result if to consider it along a curve but not a straight line.

A scenario changes when a particle hits the border of the well with nonzero tangent momentum, $\delta E \neq 0$. Then an individual trajectory, related to the regime of Eq. (10) and shown by the arrowed curve in Fig. 4, is impossible at least in a vicinity of the well where a tangent component of the momentum is finite

$$\frac{\partial S}{\partial y} \simeq \hbar B \sqrt{\delta E - V_0(y)} \tag{11}$$

and the imaginary momentum in the x direction is

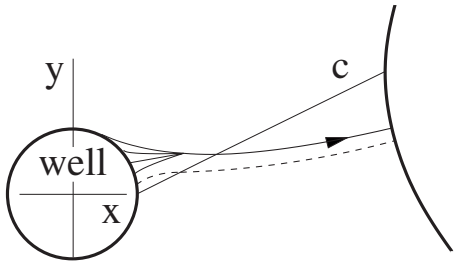

FIG. 4. Underbarrier paths at $\delta E \neq 0$ connecting two classically allowed domains as in Fig. 3. A finite tangent component results in the multipath region close to the well which goes over into the subsequent path indicated by the arrowed curve. The main path of Fig. 3 is shown by the dashed curve.

$$\frac{\partial iS}{\partial x} \simeq -\hbar B\sqrt{V_0(x) - E + \delta E}. \tag{12}$$

In this case an attempt to adjust a classical trajectory to a tangent component at the well border results in a deviating curve similar to the dashed one in Fig. 3. Therefore an underbarrier density cannot be localized on a particular classical trajectory along the entire underbarrier region. Close to the well that trajectory goes over into a wide set of paths as shown schematically in Fig. 4. According to Feynman,[36] the state related to Eqs. (11) and (12) is a superposition of a wide set of classical paths.

One can note that in a one-dimensional case, when a Hamiltonian is of a higher order than quadratic in momentum, a few underbarrier paths are also possible.[37,38] Interference of those paths may result in an oscillatory density under the barrier.

As follows from Eq. (12), a finite δE reduces the wave function in a vicinity of the well. In contrast, far from the well the wave function $\exp(iS_{cl}/\hbar)$ on the arrowed curve in Fig. 4 is larger compared to the dashed curve ($\delta E=0$) since the former is closer to the line c where $V(x,y)$ is smaller. In other words, the arrowed curve in Fig. 4 is shifted to a more transparent part of the barrier.

When the energy E is close to the bottom of the well the fraction of the trajectory above the curve c in Fig. 3 is small because the well shrinks. As follows from above, there are two opposite effects on tunneling when the total energy in the well is redistributed between a normal $(E-\delta E)$ and a tangent (δE) motions. (i) The reduction in tunneling is connected to a vicinity of well where the wave function is suppressed due to a reduction in an energy level down to $E-\delta E$. As follows from Eq. (12), the exponential reduction in the particle density is $\exp(-c_1 B\delta E)$, where c_1 is a positive parameter. (ii) The enhancement of tunneling is due to a shift of the subsequent trajectory to a more transparent part of the barrier. A reduction in $V(x,y)$ in that region is proportional to αxy. Since a typical $x\sim 1$ and $y\sim\sqrt{\delta E}$, the exponential enhancement of the particle density, according to Eq. (10), can be estimated as $\exp(2c_2 B\alpha\sqrt{\delta E})$, where c_2 is a positive parameter.

A total effect on the tunneling probability $\Gamma(\delta E)$ is defined by a product of the two exponents

$$\Gamma(\delta E) \sim \Gamma(0)\exp(-c_1 B\delta E)\exp(2c_2 B\alpha\sqrt{\delta E}). \tag{13}$$

At $\delta E\sim\alpha^2$ the expression (13) reaches a maximum, $\Gamma(0)\exp(B\alpha^2 c_2^2/c_1)$, which manifests an exponential enhancement of tunneling due to a finite δE. The parameters c_1 and c_2 are approximately of the order of unity. Whereas α is small the semiclassical combination $B\alpha^2$ is large. It is amazing, that the above conclusions, drawn on the basis of general arguments, are confirmed (excepting some details) by exact calculation in Sec. IV where the values of c_1 and c_2 are specified.

C. Analogy with photon-assisted tunneling

Multipath tunneling through a two-dimensional static barrier is similar to photon-assisted tunneling across a nonstationary one-dimensional barrier.[39] The latter also consists of two parts. The first one is an absorption of quanta with an exponentially small probability analogous to the first exponent in Eq. (13). The second one is tunneling in a more transparent part of the barrier (a higher energy) with an enhanced probability corresponding to the second exponent in Eq. (13). A total probability is also determined by a maximum of the product. In the both cases a particle finds a more transparent part of a barrier being initially pushed either by a tangent motion (at the end of the multipath region in Fig. 4) or by quanta absorption.

IV. UNDERBARRIER WAVE FUNCTION IN A SYMMETRIC SQUID

To quantitatively study the problem of two-dimensional tunneling one should solve the Schrödinger equation with the exact potential [Eq. (8)]. Since the potential barrier is almost classical one can apply a semiclassical method. With an exponential accuracy the wave function is

$$\psi \sim \exp(iB\sigma\sqrt{2}), \tag{14}$$

where the exponent is a large classical action measured in the units of Planck's constant. As follows from Eq. (6), $\sigma(x,y)$ satisfies the Hamilton-Jacobi equation[10,35]

$$\left(\frac{\partial\sigma}{\partial x}\right)^2 + \left(\frac{\partial\sigma}{\partial y}\right)^2 + V_0(x) + V_0(y) - f(x)y = E, \tag{15}$$

where $f(x)=2\alpha x/(1+\alpha)$. When $\alpha=0$ the variables in Eq. (15) are separated and a solution can be easily obtained. In our case there a substantial cross term $f(x)y$ in Eq. (15) which mixes the modes.

We consider a small coupling α when a deviation of the variable y from the tunneling path is small. For convenience, below a model coupling between the variables x and y is introduced. Namely, instead of the linear in x function we use

$$f(x) = \begin{cases} 0 & x < x_0 \\ 2\alpha & x_0 < x, \end{cases} \tag{16}$$

where x_0 is chosen between a_2 and a_1 in Fig. 1. The choice of this form, Eq. (16), does not contradict to main arguments of Sec. III.

A. Hamilton-Jacobi approach

At a small coupling, $\alpha \ll 1$, we consider a transition through the barrier along the direction x. The transition occurs with a small deviation of y from zero position. In this case one can put $V_0(y)=y^2$ in Eq. (15). The classically allowed motion in the well $V_0(x)+y^2<E$ is described by a real action $\sigma(x,y)$. The particle probes the potential in the classically allowed region where motions in x and y directions are independent. Therefore the level quantization is determined by two one-dimensional wells and the action is a sum of two one-dimensional parts defined by a solution of Eq. (15) with the condition (16) at $x<x_0$. A continuation of this action from the well to under the barrier at $x<x_0$ results in

$$\sigma(x,y) = i\int_{x_0}^{x} dx_1 \sqrt{V_0(x_1) - E + \delta E} + \int_0^y dy_1 \sqrt{\delta E - y_1^2}. \tag{17}$$

The part δE of the total energy E relates to the tangent (perpendicular to the tunneling direction) motion. The fraction δE is determined by a state in the well from which tunneling occurs. At a large B the energies E and δE are almost continuous with a discreetness $1/B$.

A solution at $x_0<x$ can be found by the method of variation of constants.[35] It has the form

$$\sigma(x,y) = i\int_{x_0}^{x} dx_1 \sqrt{V_0(x_1) - E - \alpha^2 + \varepsilon(x,y)} + \int_{\alpha}^{y} dy_1 \sqrt{\varepsilon(x,y) - (y_1 - \alpha)^2} + iF[\varepsilon(x,y)], \quad x_0 < x. \tag{18}$$

For a given function $F(\varepsilon)$ the function $\varepsilon(x,y)$ is determined by the condition $\partial\sigma/\partial\varepsilon=0$

$$2i\frac{\partial F(\varepsilon)}{\partial \varepsilon} = i\int_{x_0}^{x} \frac{dx_1}{\sqrt{V_0(x_1) - E - \alpha^2 + \varepsilon}} + \int_{\alpha}^{y} \frac{dy_1}{\sqrt{\varepsilon - (y_1 - \alpha)^2}}, \tag{19}$$

which is independence of σ on "constant" $\varepsilon(x,y)$. Now derivatives of the action have the simple forms

$$\frac{\partial \sigma(x,y)}{\partial x} = i\sqrt{V_0(x) - E - \alpha^2 + \varepsilon(x,y)},$$

$$\frac{\partial \sigma(x,y)}{\partial y} = \sqrt{\varepsilon(x,y) - (y-\alpha)^2}. \tag{20}$$

According to matching of $\partial\sigma(x_0,y)/\partial y$ given by Eqs. (17) and (18), $\varepsilon(x_0,y)=\delta E+\alpha^2-2\alpha y$. This can be used to determined the function $F(\varepsilon)$ if to express y through $\varepsilon(x_0,y)$ and to insert that into Eq. (19). As a result, the function $\varepsilon(x,y)$ is defined by the condition

$$i\int_{x_0}^{x} \frac{dx_1}{\sqrt{V_0(x_1) - E - \alpha^2 + \varepsilon}} = \int_{y-\alpha}^{(\delta E - \alpha^2 - \varepsilon)/2\alpha} \frac{dz}{\sqrt{\varepsilon - z^2}}. \tag{21}$$

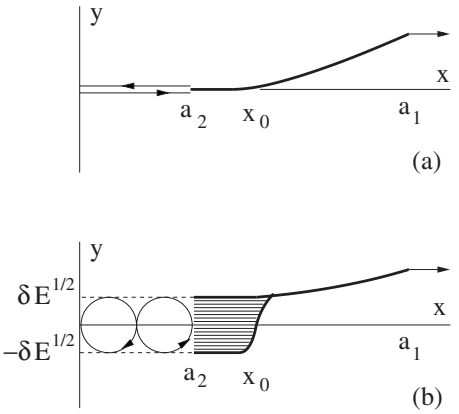

FIG. 5. At the region $a_2<x<a_1$ the motion is classically forbidden. (a) Tunneling from a state with zero tangent momentum, $\delta E=0$. A particle density is localized on the thick curve which is the main path. (b) Tunneling from a state with nonzero tangent momentum, $\delta E\neq 0$. At each fixed x from the interval $a_2<x<x_0$ the modulus of the wave function is a constant, within the exponential accuracy, at the entire dashed (multipath) region. Classical trajectories at the well, $x<a_2$, are shown.

B. Probability of tunneling

Not very close to the classical exit point a_1, determined by the condition $V_0(x)\simeq E$, one can write the left hand side of Eq. (21) as $i\tau(x)$, where

$$\tau(x) = \int_{x_0}^{x} \frac{dx_1}{\sqrt{V_0(x_1) - E}}. \tag{22}$$

Now a solution of Eq. (21) can be easily obtained. At $x_0<x$

$$\sqrt{(y-\alpha)^2 - \varepsilon} = \sqrt{(y + 2\alpha \sinh^2 \tau/2)^2 - \delta E} - \alpha \sinh \tau. \tag{23}$$

There is a remarkable underbarrier path, $y(x)$, where $\partial\sigma(x,y)/\partial y=0$. According to Eq. (20), at $x_0<x$

$$y(x) = \sqrt{\alpha^2 \sinh^2 \tau(x) + \delta E} - \alpha[\cosh \tau(x) - 1]. \tag{24}$$

The path $y(x)$ is shown in Fig. 5 by thick curves. In Fig. 5(b) this is the upper curve.

The region $x<a_2$ in Fig. 5 pertains to the classical motion in the well. At the classically forbidden region, $a_2<x<a_1$, the wave function strongly depends on δE. At $\delta E=0$ the wave function is localized at a close vicinity of the curve $y(x)$ in Fig. 5(a) (main-path tunneling).

At $\delta E\neq 0$ the wave function is localized on the curve $y(x)$ at its part $x_0<x<a_1$ only. At the underbarrier region $a_2<x<x_0$ the regime is different. At each fixed x the modulus of the wave function is a constant, with the exponential accuracy, along the wide dashed region shown in Fig. 5(b) (multipath tunneling). At a finite δE there are real momenta under the barrier according to Eq. (17). At $x=a_1$ the particle escapes from under the barrier.

Below it is convenient to introduce

$$\mu(x) = \varepsilon[x, y(x)]. \tag{25}$$

As follows from Eqs. (23) and (24)

$$\sqrt{\mu(x)} = \alpha \cosh \tau(x) - \sqrt{\alpha^2 \sinh^2 \tau(x) + \delta E}. \tag{26}$$

We define probability of tunneling with a fixed energy E and an exchange δE as

$$\Gamma(\delta E) = \left| \frac{\psi[a_1, y(a_1)]}{\psi(a_2, 0)} \right|^2 \sim \exp\left(2iB\sqrt{2} \int_{a_2}^{a_1} \frac{\partial \sigma[x, y(x)]}{\partial x} dx \right). \tag{27}$$

The definition, Eq. (27), is analogous to Eq. (13). It is useful to consider the probability of tunneling $\Gamma(0)$ at $\delta E = 0$. To obtain it one has to expand the root in the first Eq. (20) with respect to $\varepsilon - \alpha^2$ and to substitute into Eq. (27). With the use of Eqs. (25) and (26) we obtain

$$\Gamma(0) = \Gamma_{\mathrm{WKB}} \exp\left\{ \frac{B\alpha^2}{\sqrt{2}} [2\tau(a_1) - 1 + e^{-2\tau(a_1)}] \right\}, \tag{28}$$

where

$$\Gamma_{\mathrm{WKB}} \sim \exp\left[-2B\sqrt{2} \int_{a_2}^{a_1} dx \sqrt{V_0(x) - E} \right] \tag{29}$$

is a one-dimensional WKB-like expression.

C. Tunneling from a state with nonzero tangent momentum, $\delta E \neq 0$

We consider weak tangent momenta related to the condition $\delta E \sim \alpha^2$. According to Eqs. (20), (26), and (27), at $\delta E \ll \alpha^2$ the tunneling probability is

$$\Gamma(\delta E) = \Gamma(0) \exp\left(-B\delta E\sqrt{2} |\tau(a_2)| + \frac{B\delta E}{\sqrt{2}} \ln \frac{\alpha^2}{\delta E} \right). \tag{30}$$

The first term in the exponent comes from a conventional WKB reduction in tunneling probability at $x < x_0$ when the energy is reduced by δE. The second term in the exponent is due to the region $x_0 < x$ where the trajectory goes in a more transparent part of the barrier. The second term dominates at $\delta E \ll \alpha^2$ and increases the tunneling probability.

As follows from Eq. (26), at δE close to α^2, $\mu(x) = (\alpha - \sqrt{\delta E})^2 / \cosh^2 \tau(x)$. This means that the increase of the tunneling probability, associated with the region $x_0 < x$, is more effective at $\delta E = \alpha^2$. According to Sec. III, when E is not far from the well bottom the crossover between two regimes is shifted toward the point $x = a_2$. For this reason, below we choose the parameter x_0 in Eq. (16) to be close to a_2 for simplicity. In this case, at δE close to α^2, the tunneling probability is

$$\Gamma(\delta E) = \Gamma(0) \exp\left\{ \frac{B\alpha^2}{\sqrt{2}} \left[1 - e^{-2\tau(a_1)} - \frac{2}{\alpha^2} (\alpha - \sqrt{\delta E})^2 \tanh \tau(a_1) \right] \right\}. \tag{31}$$

There is another expression of the probability which follows from Eqs. (28) and (31)

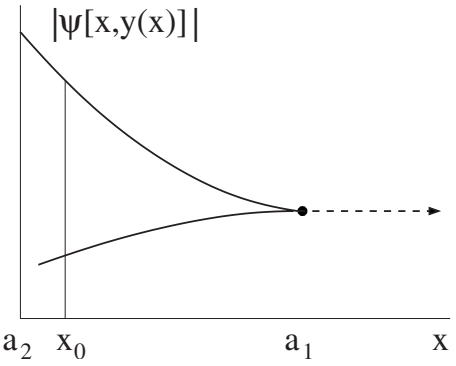

FIG. 6. Modulus of the wave function at $\delta E = \alpha^2$. In this case $y(x) = \alpha$ at all $a_2 < x < a_1$.

$$\Gamma(\delta E) = \Gamma_{\mathrm{WKB}} \exp\left\{ B\alpha^2\sqrt{2} \left[\tau(a_1) - \frac{(\alpha - \sqrt{\delta E})^2}{\alpha^2} \tanh \tau(a_1) \right] \right\}. \tag{32}$$

The Gaussian form, Eq. (32), is analogous to Eq. (13). The tunneling probability reaches a maximum at $\delta E = \alpha^2$ as it has been predicted in Sec. III. The modulus of the wave function is plotted in Fig. 6, where $y(x) = \alpha$ for all underbarrier track, $a_2 < x < a_1$. There are two branches under the barrier and an outgoing wave after the exit indicated by the dashed line in Fig. 6.

D. A relation between semiclassical approximation and WKB

In semiclassical approximation the wave function in a problem of any dimension has the form[10]

$$\psi \sim \exp(iS/\hbar), \tag{33}$$

where S is a classical action satisfying Hamilton-Jacobi equation.[35]

In the original papers by Wentzel,[7] Kramers,[8] and Brillouin[9] a static one-dimensional potential was considered when the only solution of the Hamilton-Jacobi equation was $S = \int p dx$. This phase integral constitutes the basis of WKB approach. So in a static one-dimensional case semiclassical approximation is equivalent to WKB.

In a multidimensional case a situation is more complicated. First, there are solutions of the Hamilton-Jacobi equation when a wave function under the barrier is localized on the certain trajectory $\vec{l}(\vec{r})$ (main path) in the multidimensional space. The wave function decays along the main path according to the form $S = \int \vec{p} d\vec{l}$ where $\vec{p}$ is imaginary. This phase integral is analogous to one in the one-dimensional problem if to substitute a straight path by the curve $\vec{l}(\vec{r})$. Therefore, in this case semiclassical approximation and WKB are similar. An example of this situation is Fig. 5(a).

Second, some solutions of the Hamilton-Jacobi equation are possible when the wave function is not localized on the certain underbarrier trajectory. An example of this type is Fig. 5(b) where the wave function is smeared out over a wide (multipath) domain. This is an example of semiclassical ap-

proximation which is not generic with a WKB-like phase integral along a main path. See also Ref. 34. Therefore we distinguish between the terms "semiclassical approximation" and "WKB."

V. TUNNELING IN A SYMMETRIC SQUID AT FIXED TEMPERATURE AND CURRENT

For comparison with experiments one should express the tunneling probability in terms of temperature and current.

A. Temperature dependence of tunneling probability

At a fixed particle energy E a tunneling probability is determined by Eqs. (29) and (32) with $\delta E=\alpha^2$. At a fixed temperature all energies contribute to tunneling with Gibbs factors $\exp(-E_0/T)$. In the semiclassical limit, $1 \ll B$, there are many levels in the well. Therefore one can treat E as a continuous variable and to optimize the probability $\Gamma(\delta E)\exp(-E_0/T)]$ with respect to E accounting for Eq. (9). This procedure gives the certain optimal energy E_T from which tunneling occurs.[2,3,28–31] If to omit the term proportional to α^2 in $\Gamma(\delta E)$, Eq. (32), an optimal energy E_T is determined by

$$\tau(a_1)=\frac{\hbar}{t_0 T\sqrt{2}}. \tag{34}$$

Imaginary time $\tau(a_1)$ is given by Eq. (22) where one should put now $x_0=a_2$. It follows that at $T=0$ the optimal energy is $E_T=0$. E_T at the barrier top in Fig. 2 corresponds, at small α, to the critical temperature $T_0=\hbar/\pi t_0\sqrt{2}$ when the decay occurs solely due to thermal activation.

Now one can express the tunneling probability Γ_T at a fixed temperature in the form

$$\Gamma_T=\Gamma_T^{(0)}\exp\left\{\frac{B\alpha^2}{\sqrt{2}}\left[1-\exp\left(-\frac{2\pi T_0}{T}\right)\right]\right\}, \tag{35}$$

where the exponential coincides with one of Eq. (31) if to insert there $\delta E=\alpha^2$ and the expression (34). $\Gamma_T^{(0)}$ is a probability of a conventional tunneling when a tangent momentum in the well is zero. As follows from the expression (35), $\Gamma_T^{(0)}<\Gamma_T$. This means that tunneling occurs from states with a finite tangent momentum. Since energy E has to be larger than $\delta E(=\alpha^2)$ temperature cannot be too low, $1/\ln(1/\alpha)<T/T_c<1$.

B. Dependence of tunneling probability on current

Let us consider first an almost continuous distribution of levels in the well ($1 \ll B$). The coupling constant α is of the order of unity at $I=I_R$, where

$$\left(1-\frac{I_R}{2I_c}\right)=\frac{1}{\beta^2}. \tag{36}$$

Since currents are close to the critical value $2I_c$ the parameter β is supposed to be large. A dependence of Γ_T on current is schematically shown in Fig. 7. The limit of a small α, considered above and defined by Eq. (35), corresponds to the left part of the curves in Fig. 7. Parts of the curves in Fig. 7 closer to $2I_c$ pertain to a large α. In this case tunneling occurs symmetrically, $x=y$, since a deviation from this path costs a lot of energy.[20]

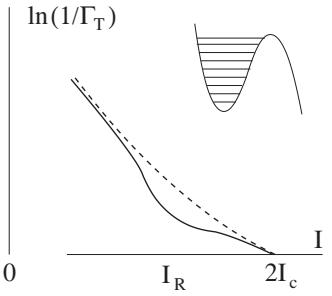

FIG. 7. Dependence of tunneling probability at a fixed temperature Γ_T on current in the case of an almost continuous distribution of levels in the well (see inset). The dashed curve corresponds to the conventional probability $\ln(1/\Gamma_T^{(0)})$.

The dashed curve in Fig. 7 is $\Gamma_T^{(0)}$. It is very easy to numerically calculate $\Gamma_T^{(0)}$ using a standard technique[20] when a two-dimensional trajectory is normal to classically allowed regions.[2,3,27–31] $\Gamma_T^{(0)}$ depends on parameters (coupling strength, asymmetry of junctions, etc.) of a SQUID fabricated for measurements. For comparison with experiments one has to know those values exactly. For this reason, we leave $\Gamma_T^{(0)}$ as a schematic dashed curve in Fig. 7 planning its exact calculation in the nearest future for particular parameters of a SQUID with an intermediate effective coupling.

The curves in Fig. 7 are taken at a fixed temperature which exceeds $T_0=[2(1-I/I_c)]^{1/4}\hbar\omega/2\pi$ sufficiently close to $2I_c$ (large α).[20] In other words, in a close vicinity of $2I_c$ the decay is due to a thermal activation. We will consider details elsewhere.

When the semiclassical parameter B is not too large a tunneling probability still remains exponentially small but a level distribution in the well becomes substantially discrete. This is a typical experimental situation.[11–14] The underbarrier process sets the certain energy $\delta E=\alpha^2$ which is given up to the tangent motion. According to Eq. (31), the tunneling probability reaches a maximal value under that condition. The energy exchange is similar to one illustrated in Fig. 2.

On the other hand, the optimal δE may not be exactly fitted by discrete energy levels in the well which can be outside the Gaussian distribution [Eq. (31)]. This contrasts to a continuous distribution of levels at a large B when a proper level always exists. A mismatch between δE and the level structure results in reduction in the tunneling probability.

For this reason, one can expect a "resonance" due to coincidence of $\delta E(=\alpha^2)$ with a distance between discrete levels. There are no sharp peaks but rather a shallow wavy structure in Γ_T illustrated in Fig. 8. Each minimum results from the resonance and is smeared out at the interval of currents

$$\frac{\delta I}{2I_c-I_R}\sim\frac{1}{\sqrt{B}}, \tag{37}$$

which follows from the Gaussian distribution in Eq. (31). Under the condition (36) a depth of each minimum in Fig. 8

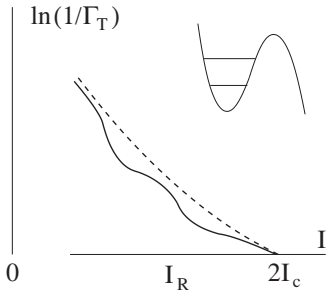

FIG. 8. Dependence of tunneling probability at a fixed temperature Γ_T on current in the case of discrete levels in the well (see inset). The dashed curve is the same as in Fig. 7.

is on the order of one. In Fig. 8 only two minima are shown. Strictly speaking, the semiclassical theory is not applicable to a case of moderate B and the above arguments are heuristic.

VI. TUNNELING IN AN ASYMMETRIC SQUID

Below, in Secs. VI–IX, we consider the case of a very asymmetric SQUID, $1 \ll M$, when the coordinate φ_2 in Eq. (2) is heavy. A character of tunneling in an asymmetric case also depends on coupling strength α between the two junctions. At $\alpha=0.90$ the curves of equal potential, $V(x,y)=E$, are shown in Fig. 9. An effective particle tunnels from one classically allowed region (the potential well) to another (the outer region).

To quantitatively study the problem of two-dimensional tunneling one should solve the Schrödinger equation with the exact potential in Eq. (8). Since the potential barrier is almost classical one can apply a semiclassical method when a wave function has the form

$$\psi \sim \exp(iB\sigma), \tag{38}$$

where the classical action is $\hbar B\sigma$. σ satisfies the equation of Hamilton-Jacobi[10]

$$\frac{1}{2}\left(\frac{\partial\sigma}{\partial x}\right)^2 + \frac{1}{2M}\left(\frac{\partial\sigma}{\partial y}\right)^2 + V(x,y) = E. \tag{39}$$

We define the energy E by the relation

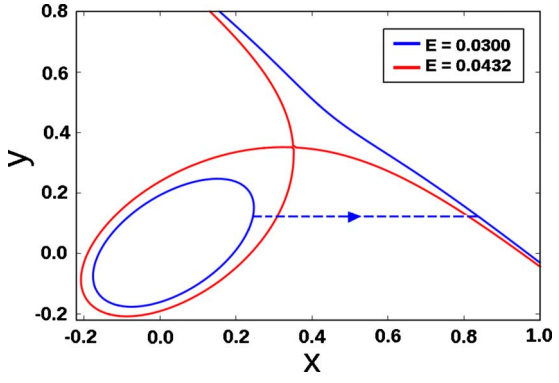

FIG. 9. (Color online) Curves of a constant energy $V(x,y)=E$ at $\alpha=0.9$. Tunneling occurs along the dashed line, $y=y_0$, where an underbarrier wave function is localized.

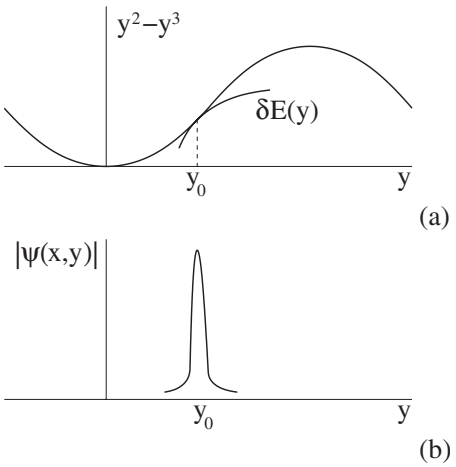

FIG. 10. (a) Form of $\delta E(y)$. (b) Corresponding density distribution is Gaussian. It is plotted for some x under the barrier.

$$E_0 = \frac{\hbar B}{t_0}. \tag{40}$$

At a large M a solution of Eq. (39) can be written in the form $\sigma=\sigma_0+\sigma_1$, where σ_1 is small and σ_0 is given by

$$\frac{\sigma_0(x,y)}{\sqrt{2}} = i\int^x dx_1 \sqrt{x_1^2 - x_1^3 - \frac{2\alpha x_1 y}{1+\alpha} - E + \delta E(x_1,y)} + \sqrt{M}\int^y dy_1 \sqrt{\delta E(x,y_1) - y_1^2 + y_1^3}, \tag{41}$$

where $\delta E(x,y)$ is some function to be specified. It is easy to conclude that the correction σ_1 is small (proportional to $1/\sqrt{M}$) when the derivative $\partial\delta E/\partial x$ is small (proportional to $1/M$). So we consider below $\delta E(y)$.

The function $\delta E(y)$ is determined by a state in the well from which tunneling occurs. When the case of Fig. 10(a) is realized the last term in Eq. (41) provides a Gaussian distribution of density around the line $y=y_0$ shown in Fig. 10(b) for some x under the barrier. This is analogous to a conventional scenario of tunneling in two dimensions (main path).[30,31]

In the case of $\delta E(y)$ of Fig. 11(a) at $y_0<y$, due to the second term in Eq. (41), the density drops down under the barrier as $\exp[-c(y-y_0)^{3/2}]$, where $c\sim\sqrt{M}$. At $y<y_0$ a decay of the density is provided by the first term of σ_0 in Eq. (41) so a maximum of the density is reached at $y=y_0$. At $y<y_0$ there is an additional branch of the wave function with the opposite sign of the second term in Eq. (41) related to the opposite current in the y direction. This compensates a large current in the y direction provided by the second term in Eq. (41) at $y<y_0$. Therefore the density becomes oscillatory at $y<y_0$ as shown in Fig. 11(b) for some x under the barrier.

The situations in Figs. 10 and 11 relate to different types of states in the potential well from which tunneling occurs. In the case of Fig. 10 a Gaussian distribution of density holds in the well because the last term in Eq. (41) dominates. In the case of Fig. 11 the distribution in the well is also oscillatory.

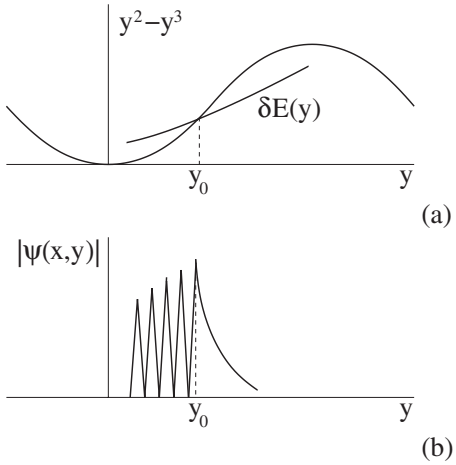

FIG. 11. (a) Form of $\delta E(y)$. (b) Corresponding density distribution, plotted for some x under the barrier, is not Gaussian. See the text.

We do not analyze here details of the wave function in the well.

As follows, in the both cases, Figs. 10 and 11, tunneling occurs along the certain line $y=y_0$ (Fig. 9) corresponding to classical mechanics when a particle does not move along a heavy direction. The line $y=y_0$ is main path in spite of a density distribution around the path can be non-Gaussian as in Fig. 11(b). A position of y_0 should be determined from the condition of maximum of a tunneling probability. With an exponential accuracy a tunneling probability is the same for the both cases.

VII. TUNNELING PROBABILITY IN AN ASYMMETRIC SQUID

Since tunneling occurs along the line $y=y_0$ one can use a WKB approach as in a one-dimensional case. The probability of tunneling with a fixed energy E is

$$\Gamma(E) \sim \exp[-2BA(E)], \tag{42}$$

where

$$A(E) = \sqrt{2}\int dx\sqrt{v(x)-E}. \tag{43}$$

The one-dimensional potential $v(x)$ is given by

$$v(x) = x^2 - x^3 - \frac{2\alpha y_0}{1+\alpha}x + y_0^2 - y_0^3. \tag{44}$$

The integration in Eq. (43) is restricted by the classically forbidden region where $E<v(x)$.

Tunneling probability at a fixed temperature accounts for the Gibbs factor and is determined by

$$\Gamma \sim \exp\left[-2BA(E) - \frac{E_0}{T}\right] \tag{45}$$

with a subsequent optimization with respect to E. Taking Eq. (40), one can write Eq. (45) in the form

$$\Gamma \sim \exp(-2BA_T), \tag{46}$$

where

$$A_T = A(E) + \frac{E}{\theta}. \tag{47}$$

The parameter θ is connected with temperature

$$\theta = \frac{2T\sqrt{\beta}}{\hbar\omega}\sqrt{\frac{2\alpha}{1+\alpha}}. \tag{48}$$

Minimization of A_T with respect to energy defines E by the equation

$$\frac{1}{\theta} = \frac{1}{\sqrt{2}}\int \frac{dx}{\sqrt{v(x)-E}}. \tag{49}$$

The parameter y_0 should be chosen to minimize A_T.

By introducing imaginary time $t=i\tau$ the action A_T can be written in the form

$$A_T = \int_0^{1/\theta} d\tau\left[\frac{1}{2}\left(\frac{\partial x}{\partial \tau}\right)^2 + v(x)\right], \tag{50}$$

where the classical trajectory under the barrier is determined by Newton's equation

$$\frac{\partial^2 x}{\partial \tau^2} = 2x - 3x^2 - \frac{2\alpha y_0}{1+\alpha} \tag{51}$$

with zero velocities at the terminal points, $\tau=0$ and $\tau=1/\theta$. According to Eq. (49), $1/\theta$ is the underbarrier time of motion between two terminal points. In terms of trajectories, the condition of minimum A_T with respect to y_0 takes the form

$$2y_0 - 3y_0^2 = \frac{2\alpha\theta}{1+\alpha}\int_0^{1/\theta} x d\tau. \tag{52}$$

For a strongly asymmetric SQUID, a large M, tunneling occurs along a straight line $y=y_0$ shown in Fig. 9. The action in Eq. (50) depends on two parameters, α and $T\sqrt{\beta}/\hbar\omega$.

The tunneling probability satisfies the relation

$$\frac{1}{B_0}\ln\frac{1}{\Gamma} = \sqrt{2}\left(\frac{1+\alpha}{\alpha}\right)^{5/2} A_T(\alpha, T\sqrt{\beta}/\hbar\omega). \tag{53}$$

A recipe of calculation of the action A_T is the following. At fixed α, y_0, and θ one should find a solution of Eq. (51) with zero velocities, $\partial x/\partial\tau=0$, at $\tau=0,1/\theta$. That solution has to be inserted into the relation (52) which defines y_0 at fixed θ and α. The solution with the defined y_0 should be substituted into Eq. (50) which produces $A_T(\alpha, T\sqrt{\beta}/\hbar\omega)$. We demonstrate in Sec. VIII how this scheme works in the case of low temperatures.

VIII. TUNNELING AT LOW TEMPERATURES IN AN ASYMMETRIC SQUID

At low temperatures the energy E should be close to the minimum of the potential $v(x)$ providing a long underbarrier time $1/\theta$. With the value of energy

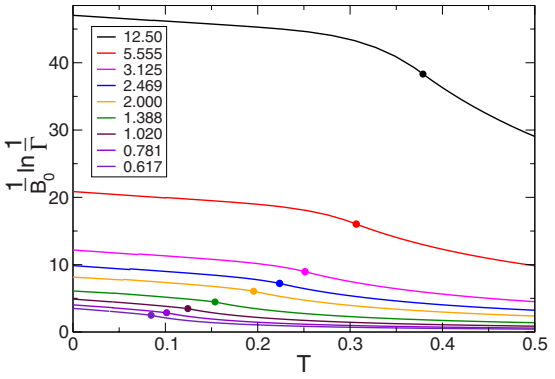

FIG. 12. (Color online) Γ is tunneling probability in an asymmetric SQUID. Temperature T is measured in the units of $\hbar\omega/\sqrt{\beta}$. The numbers mark values of the parameter $(1-j)\beta^2$.

$$E = \frac{1+2\alpha}{(1+\alpha)^2} y_0^2 \tag{54}$$

the action takes the form

$$A_T = \frac{4\sqrt{2}}{15} - \frac{2\sqrt{2}\alpha y_0}{1+\alpha} + \frac{E}{\theta}. \tag{55}$$

A minimization with respect to y_0 of the action in Eq. (55), accounting for Eq. (54), is equivalent to Eq. (52). The resulting action, at low dimensionless temperature θ, is

$$A_T = \frac{4\sqrt{2}}{15} - \frac{2\alpha^2}{1+2\alpha}\theta. \tag{56}$$

IX. RESULTS FOR AN ASYMMETRIC SQUID

We performed a numerical solution of Eq. (51). The results for the tunneling probability are presented in Figs. 12 and 13 where temperature T is measured in the units of $\hbar\omega/\sqrt{\beta}$. Each curve in Figs. 12 and 13 consists of two parts. To the left of a dot each curve relates to above trajectory calculations corresponding to thermally assisted tunneling. To the right of a dot a curve is solely due to thermal activation

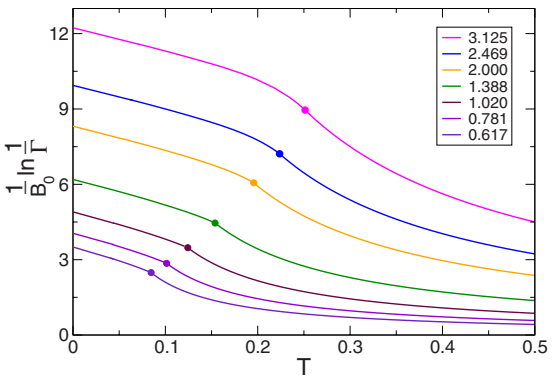

FIG. 13. (Color online) Amplification of the lower set of curves in Fig. 12 for an asymmetric SQUID. Left parts of the curves relate to a thermally assisted tunneling and right parts pertain to pure activation.

$$\frac{1}{B_0}\ln\frac{1}{\Gamma} = \frac{\hbar\omega}{T\sqrt{\beta}}\frac{2}{27\alpha^3}\begin{cases}(1-\alpha)(1+2\alpha)^2 & \alpha < 1/2\\ 2 & 1/2 < \alpha.\end{cases} \tag{57}$$

The activation energy is given by the saddle point $V(x_s, y_s)$ which coincides with the crossing point of two curves in Fig. 9. The steepest descent in Fig. 9 goes along the direction $x=y$. The saddle point $\{x_s, y_s\}$ is determined by the conditions $\partial V(x,y)/\partial x = \partial V(x,y)/\partial y = 0$. At $1/2 < \alpha$

$$x_s = y_s = \frac{2}{3(1+\alpha)} \tag{58}$$

and at $\alpha < 1/2$

$$x_s, y_s = \frac{1+2\alpha \pm \sqrt{1-4\alpha^2}}{3(1+\alpha)}. \tag{59}$$

At $\alpha < 1/2$ the transition to a pure activation regime is smooth as in a one-dimensional case. It is analogous to type-II phase transition. This corresponds to $2 < (1-j)\beta^2$ in Figs. 12 and 13. At $1/2 < \alpha$ the transition to the activation regime reminds type-I phase transition. A derivative with respect to temperature jumps at those points which can be observed in Fig. 13. Appearance of the jumps is a consequence of two-dimensionality when the pure thermal activation does not smoothly go over into a thermally assisted tunneling. In this case a transition point between them corresponds to equal tunneling probabilities of two different processes. In one dimension they always merge smoothly when an optimum in energy coincides with a barrier top.

Numerically calculated curves in Figs. 12 and 13 match at low temperatures the analytical dependence followed from Eqs. (53) and (56). At low temperatures

$$\frac{1}{B_0}\ln\frac{1}{\Gamma} = \frac{8}{15}\left(\frac{1+\alpha}{\alpha}\right)^{5/2}\left[1 - \frac{T\sqrt{\beta}}{\hbar\omega}\frac{15\alpha^2\sqrt{\alpha}}{(1+2\alpha)\sqrt{1+\alpha}}\right]. \tag{60}$$

We note that the slope in the temperature dependence in Eq. (60) is finite at low temperatures. It is a consequence of two-dimensionality since the activation energy E in that case is proportional to T^2. In one dimension it is exponentially small as $\exp(-\text{const}/T)$. This is due to proportionality of a period of oscillations in one dimension, which is $\hbar/T$, to $\ln 1/E$ as follows from classical mechanics.[35]

The tunneling probability Γ as a function of the parameter $(1-j)\beta^2$ is plotted in Fig. 14 for different values of the dimensionless temperature $T\sqrt{\beta}/\hbar\omega$. This plot shows how Γ depends on current at a fixed temperature.

X. DISCUSSIONS

Scenario of tunneling in a SQUID substantially depends on that whether it is almost symmetric ($M \sim 1$) or very asymmetric ($1 \ll M$). A diagram of regimes, considered in the paper, is sketched in Fig. 15 in the plane of asymmetry parameter M and coupling parameter α. We discuss first an almost symmetric SQUID. In that case effects of two-dimensionality can be strongly pronounced.

Quantum tunneling across a one-dimensional static potential barrier is described by WKB theory. Tunneling through a

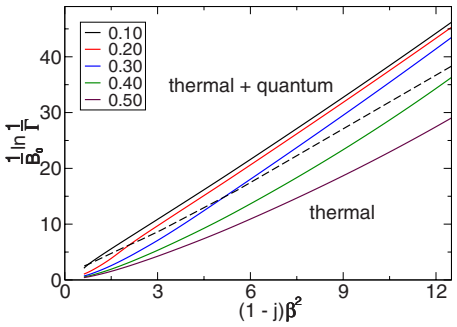

FIG. 14. (Color online) Tunneling probability Γ (for an asymmetric SQUID) versus current for various values of the dimensionless temperature $T\sqrt{\beta}/\hbar\omega$. The dashed curve separates thermally assisted tunneling from a pure thermal activation.

multidimensional barrier is well studied.[28–31] Accordingly, the main contribution to a tunneling probability comes from the extreme path linking two classically allowed regions. The path is a classical trajectory with real coordinates which can be parametrized by imaginary time. The underbarrier trajectory is a solution of Newton's equation in imaginary time. The trajectory is given rise by a particle hitting normally (with zero tangent momentum) a border of the classically allowed region. In terms of discrete levels in the well tunneling occurs from a state with the analogous property. Under the barrier the probability density reaches a maximum at each point of the trajectory along the orthogonal direction with respect to it. Along that direction the density has a Gaussian distribution. Therefore around the trajectory, which plays a role of a saddle point, quantum fluctuations are weak. The wave function, tracked along that trajectory under the barrier, exhibits an exponential decay generic with WKB behavior. This constitutes a conventional scenario of tunneling in multidimensional case[30,31] which can be called main-path tunneling.[37] This mechanism was explored for two-dimensional tunneling in a symmetric SQUID in Ref. 20.

However, in some cases tunneling through multidimensional barriers occurs according to a different scenario which is not similar to a WKB-like phase integral along the certain path. An example of such situation in a symmetric SQUID is investigated in the paper.

When a state before tunneling has a tangent momentum with respect to a border of the well there are no extreme points on it since the derivative of the wave function along the border is finite. This means that a tunneling probability is no more determined by the main underbarrier path but comes from a wide set of paths. Traditionally, a decay of a state with a tangent momentum is not considered since it does not correspond to a saddle point and, hence, the net contribution is expected to be averaged down to a small value due to mutual interference of trajectories.

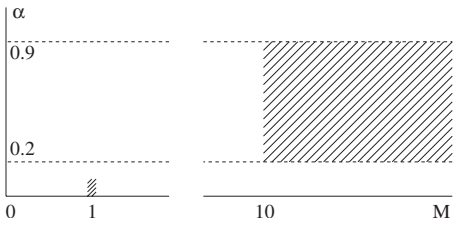

FIG. 15. A scheme of regimes of tunneling in a SQUID considered in the paper. The region in a vicinity of the point $\{M=1,\ \alpha=0\}$ corresponds to a symmetric SQUID in Secs. III–V. The dashed domain, at approximately $M>10$, relates to an asymmetric SQUID in Secs. VI–IX.

It is shown in the paper by general arguments and exact calculations that a nonzero tangent momentum does not result in reduction in tunneling probability. Moreover, a related multipath mechanism can exponentially enhance barrier penetration in a SQUID which is not very asymmetric. In contrast to main-path mechanism, multipath tunneling cannot be calculated using a classical trajectory in imaginary time. Such a trajectory, connecting two physical (real) points, does not exist in that case.

A possible way of interpretation of multipath tunneling is proposed in Sec. III. In a vicinity of an entrance under the barrier it is locally less transparent. A wide distribution of paths in that region goes over into the single path which proceeds up to an end of the barrier. That path lies in a more transparent part of the barrier resulting in enhancement of tunneling probability.

Multipath tunneling through a two-dimensional static barrier reminds photon-assisted tunneling across a nonstationary one-dimensional barrier. In the both cases a particle finds a more transparent part of a barrier being initially pushed either by a tangent motion or by quanta absorption.

The total energy E of a state in the well is distributed as $E-\delta E$ for a motion in the tunneling direction and as δE for tangent one. For a small coupling constant α the maximal tunneling probability corresponds to $\delta E \sim \alpha^2$.

An analysis of experimental data allows to define a contribution of multipath effects by separation of the conventional probability $\Gamma_T^{(0)}$ from a total result. $\Gamma_T^{(0)}$ depends on parameters (coupling strength, asymmetry of junctions, etc.) of a particular SQUID fabricated for measurements.

Usually, in order to observe tunneling in a SQUID a current should be close to the critical one to reduce the effective action. The condition for multipath tunneling is a weak coupling $(1 \ll \beta)$ between junctions in a SQUID to provide an intermediate value of the parameter α [Eq. (5)]. The effect was not observed yet since β was not sufficiently large in existing experiments.[22–24] It was $\beta \simeq 0.37$ in Ref. 22, $\beta \simeq 0.3$ in Ref. 23, and $\beta \simeq 1.6$ in Ref. 24. The calculations in the paper are performed for zero magnetic field in a SQUID but this is not a principle restriction for observation of multipath tunneling. A role of dissipation is to be studied.

We see that in a multidimensional system (a SQUID is a two-dimensional example) tunneling mechanism can be different than one traditionally considered on the basis of main path. The necessary condition for unusual tunneling is that it should start not from a ground state, otherwise an energy exchange is impossible.

One should expect a modified quantum tunneling at a finite temperature across a nonone-dimensional barrier. In this case the conventional mechanism of a periodic trajectory in imaginary time with the period $\hbar/T$ is substituted by multipath mechanism.

In a very asymmetric SQUID there is always main-path tunneling along a line perpendicular to the heavy direction. It

is amazing that a density distribution around that line can be substantially non-Gaussian depending on a state in the well from which tunneling occurs. Regardless of a type of that state the tunneling exponent is the same. In a very asymmetric SQUID a barrier penetration is analogous to one-dimensional tunneling when the heavy junction is at rest. There is a continuous set of such paths in two dimensions and one should choose only one of them which provides a maximum of tunneling probability. Therefore, in a very asymmetric SQUID the problem is not completely one-dimensional.

We used a semiclassical approximation when there are many levels in the well. This approach sometimes is not appropriate in one-dimensional Josephson junctions where a barrier is weakly transparent but nevertheless there is only a few levels in the well (say, five).[5,6,11–13] In a SQUID based on two such junctions the number of levels can be roughly estimated as 5×5. In our case of a strongly asymmetric SQUID that number should be multiplied by the large parameter $\sqrt{M}$. Therefore the approximation of a large number of levels in the well is reasonable.

We propose two peculiarities of tunneling in a very asymmetric SQUID which do not exist in a single junction and in a not very asymmetric SQUID. One of them is temperature dependence of tunneling probability at low temperature. According to Eq. (60), the curves in Fig. 13 have a finite slope at low temperature. In one dimension the slope is zero due to the exponent $\exp(-\text{const}/T)$ instead of T in Eq. (60).

The second peculiarity is an unusual transition between thermally assisted tunneling and pure activation marked by dots in Fig. 13. At $2<(1-j)\beta^2$ the transition is smooth but at $(1-j)\beta^2<2$ there are jumps of slopes in Fig. 13.

Low dissipation regime and parameters $M\simeq 35$ and $\beta\simeq 15$ correspond to reality in experiments with SQUIDs and fit the developed theory. It is more convenient in experiments to obtain a set of curves as in Fig. 14 since usually measurements are run at a fixed temperature. A dependence on temperature, as in Fig. 13, also can be obtained. This would provide an experimental check of the predicted dependences on temperature and current

XI. CONCLUSION

Traditionally quantum tunneling in a static SQUID is studied on the basis of a classical trajectory in imaginary time under a two-dimensional potential barrier. The trajectory connects a potential well and an outer region crossing their borders in perpendicular directions. In contrast to that main-path mechanism, a wide set of trajectories with components tangent to the border of the well can constitute an alternative mechanism of multipath tunneling. The phenomenon is essentially nonone-dimensional. Continuously distributed paths under the barrier result in enhancement of tunneling probability. A type of tunneling mechanism (main path or multipath) depends on character of a state in the potential well prior to tunneling. A temperature dependence of the tunneling probability in a very asymmetric (different capacitances) SQUID has a finite slope at zero temperature. A transition between thermally assisted tunneling and pure activation can be not smooth depending on current through a SQUID.

ACKNOWLEDGMENTS

We thank G. Blatter, S. Butz, V. B. Geshkenbein, and A. V. Ustinov for valuable discussions.

[1] B. D. Josephson, Phys. Lett. **1**, 251 (1962).
[2] A. O. Caldeira and A. J. Leggett, Phys. Rev. Lett. **46**, 211 (1981).
[3] A. O. Caldeira and A. Leggett, Ann. Phys. (N.Y.) **149**, 374 (1983).
[4] A. I. Larkin and Yu. N. Ovchinnikov, Zh. Eksp. Teor. Fiz. **85**, 1510 (1983) [Sov. Phys. JETP **58**, 876 (1983)].
[5] M. H. Devoret, J. M. Martinis, and J. Clarke, Phys. Rev. Lett. **55**, 1908 (1985).
[6] M. H. Devoret, D. Esteve, C. Urbina, J. Martinis, A. Creland, and J. Clarke, in *Quantum Tunneling in Condensed Media*, edited by A. Leggett and Yu. Kagan (North-Holland, Amsterdam, 1992).
[7] G. Wentzel, Z. Phys. **38**, 518 (1926).
[8] H. A. Kramers, Z. Phys. **39**, 828 (1926).
[9] L. Brillouin, C. R. Acad. Sci. **183**, 24 (1926).
[10] L. D. Landau and E. M. Lifshitz, *Quantum Mechanics* (Pergamon, New York, 1977).
[11] J. M. Martinis, M. H. Devoret, and J. Clarke, Phys. Rev. Lett. **55**, 1543 (1985).
[12] J. M. Martinis, M. H. Devoret, and J. Clarke, Phys. Rev. B **35**, 4682 (1987).
[13] A. Wallraff, T. Duty, A. Lukashenko, and A. V. Ustinov, Phys. Rev. Lett. **90**, 037003 (2003).
[14] M. V. Fistul, A. Wallraff, and A. V. Ustinov, Phys. Rev. B **68**, 060504 (2003).
[15] A. J. Leggett, S. Chakravarty, A. T. Dorsey, M. P. A. Fisher, A. Garg, and W. Zwerger, Rev. Mod. Phys. **59**, 1 (1987).
[16] Y. Nakamura, Y. A. Pashkin, and J. S. Tsai, Nature (London) **398**, 786 (1999).
[17] J. R. Friedman, V. Patel, W. Chen, S. K. Tolpygo, and J. E. Lukens, Nature (London) **406**, 43 (2000).
[18] C. H. van der Wal, A. C. J. ter Haar, F. K. Wilhelm, R. N. Schouten, C. J. P. M. Harmans, T. P. Orlando, S. Lloyd, and J. E. Mooij, Science **290**, 773 (2000).
[19] Y.-C. Chen, J. Low Temp. Phys. **65**, 133 (1986).
[20] B. I. Ivlev and Yu. N. Ovchinnikov, Zh. Eksp. Teor. Fiz. **85**, 668 (1987) [Sov. Phys. JETP **66**, 378 (1987)].
[21] C. Morais Smith, B. Ivlev, and G. Blatter, Phys. Rev. B **49**, 4033 (1994).
[22] F. Sharifi, J. L. Gavilano, and D. J. Van Harlingen, Phys. Rev. Lett. **61**, 742 (1988).
[23] S. X. Li Y. Yu, Yu. Zhang, W. Qiu, S. Han, and Z. Wang, Phys. Rev. Lett. **89**, 098301 (2002).

[24] F. Balestro, J. Claudon, J. P. Pekola, and O. Buisson, Phys. Rev. Lett. **91**, 158301 (2003).
[25] M. G. Castellano, F. Chiarello, R. Leoni, F. Mattioli, G. Torrioli, P. Carelli, M. Cirillo, C. Cosmelli, A. de Waard, G. Frossati, N. Grønbech-Jensen, and S. Poletto, Phys. Rev. Lett. **98**, 177002 (2007).
[26] K. Mitra, F. W. Strauch, C. J. Lobb, J. R. Anderson, F. C. Wellstood, and E. Tiesinga, Phys. Rev. B **77**, 214512 (2008).
[27] A. U. Thomann, V. B. Geshkenbein, and G. Blatter, Phys. Rev. B **79**, 184515 (2009).
[28] C. G. Callan and S. Coleman, Phys. Rev. D **16**, 1762 (1977).
[29] S. Coleman, *Aspects of Symmetry* (Cambridge University Press, Cambridge, 1985).
[30] A. Schmid, Ann. Phys. **170**, 333 (1986).
[31] U. Eckern and A. Schmid, in *Quantum Tunneling in Condensed Media*, edited by A. Leggett and Yu. Kagan (North-Holland, Amsterdam, 1992).
[32] B. I. Ivlev and V. I. Melnikov, Phys. Rev. B **36**, 6889 (1987).
[33] B. Ivlev, arXiv:1004.0987 (unpublished).
[34] B. Ivlev, arXiv:0903.5100 (unpublished).
[35] L. D. Landau and E. M. Lifshitz, *Mechanics* (Pergamon, New York, 1977).
[36] R. P. Feynman and A. R. Hibbs, *Quantum Mechanics and Path Integrals* (McGraw-Hill, New York, 1965).
[37] B. Ivlev, Phys. Rev. A **73**, 052106 (2006).
[38] M. Marthaler and M. I. Dykman, Phys. Rev. A **76**, 010102(R) (2007).
[39] B. I. Ivlev and V. I. Melnikov, in *Quantum Tunneling in Condensed Media*, edited by A. Leggett and Yu. Kagan (North-Holland, Amsterdam, 1992).